Available online at www.sciencedirect.com
ScienceDirect
Journal of the European Ceramic Society 28 (2008) 2969–2973
www.elsevier.com/locate/jeurceramsoc

ZnBO-doped (Ba, Sr)TiO_3 ceramics for the low-temperature sintering process

Se-Ho Kim, Jung-Hyuk Koh *

Department of Electronic Materials Engineering, Kwangwoon University, Seoul, Republic of Korea

Received 17 January 2008; received in revised form 18 April 2008; accepted 25 April 2008
Available online 20 June 2008

Abstract

ZnBO-doped (Ba, Sr)TiO_3 ceramics were investigated for low-temperature co-fired ceramics (LTCCs) applications. Until now, B_2O_3 and Li_2CO_3 dopants have been commonly employed as the low-temperature sintering aids. In this paper, we suggest ZnBO as an alternative dopant to the B_2O_3 and Li_2CO_3. To reduce the sintering temperature of (Ba, Sr)TiO_3, we have added 1–5 wt.% of ZnBO to (Ba, Sr)TiO_3. ZnBO-doped (Ba, Sr)TiO_3 ceramics were respectively sintered from 750 to 1350 °C by 50 °C to confirm the sintering temperature with different dopant contents. By adding 5 wt.% of ZnBO to the (Ba, Sr)TiO_3 ceramics, the sintering temperature of (Ba, Sr)TiO_3 ceramics can be reduced to 1100 °C. From the XRD analysis, ZnBO-doped (Ba, Sr)TiO_3 has no pyro phase. By adding ZnBO dopants to (Ba, Sr)TiO_3 ceramics, both of relative dielectric permittivity and loss tangent were decreased. From the frequency dispersion of dielectric properties, the relative dielectric permittivity and loss tangent of 5 wt.% ZnBO-doped (Ba, Sr)TiO_3 were 1180 and 3.3×10^{-3}, while those of BST were 1585 and 4.8×10^{-3}, respectively.

Keywords: Low-sintering temperature; $BaSrTiO_3$; ZnBO; Dielectric permittivity; Loss tangent

1. Introduction

As developing wireless portable communication systems, the miniaturization of the passive devices has been interested greatly. Although many parts of active devices were integrated by silicon technology, passive devices are rarely integrated. Therefore, the miniaturization of electronic passive devices is of great concern by employing the low-temperature co-fired ceramics (LTCCs) process. These electronic passive devices employing LTCC technology were consisted of dielectric ceramic materials and internal metallic electrode between the layers.[1] However, it is difficult to co-fire dielectric ceramics with metallic electrodes altogether, because dielectric ceramics have high-shrinkage rate, while metallic electrode materials have no shrinkage properties.

To apply ceramic materials for LTCC applications, low-sintering temperature, high-dielectric permittivity, and low-loss tangent are required. Among the ferroelectrics, $Ba_{0.5}Sr_{0.5}TiO_3$ (hereafter BST) has especially high-dielectric permittivity and low-loss tangent.[2–4] Therefore BST has been employed as the frequency agile devices. However, BST material has relatively high-sintering temperature of 1350 °C, where metallic electrode materials such as Ag, Ni and Cu cannot be employed due to their low-evaporation temperature. Therefore the sintering temperature of BST ceramics should be lowered for LTCC applications down to 900 °C. Generally low-temperature sintered ceramic materials can be prepared by (1) mixing with glass frits[5] and (2) adding with dopants such as B_2O_3,[1] CuO,[6–7] CuV_2O_6,[8] and Li_2CO_3.[9] By combining ceramic powders with glass frits the sintering temperature can be lowered drastically, while its dielectric properties are also degraded seriously. On the other hand, doping method for LTCC applications has been also studied to expect higher relative dielectric permittivity and lower loss tangent than those of glass–ceramic materials. It is reported that dielectric permittivity is decreased and loss tangent is increased by adding dopants.[9] Since the LTCC based electronic devices are usually operated in the GHz, loss tangent play an important role for the microwave applications to obtain higher efficiency.

Until now, B_2O_3 and Li have been commonly employed for effective dopants for low-temperature sintering process especially BST materials. It was reported that Li-doped BST ceramics have low-sintering temperature but high-loss tangent.[9]

* Corresponding author.
E-mail address: jhkoh@daisy.kw.ac.kr (J.-H. Koh).

0955-2219/$ – see front matter © 2008 Elsevier Ltd. All rights reserved.
doi:10.1016/j.jeurceramsoc.2008.04.034

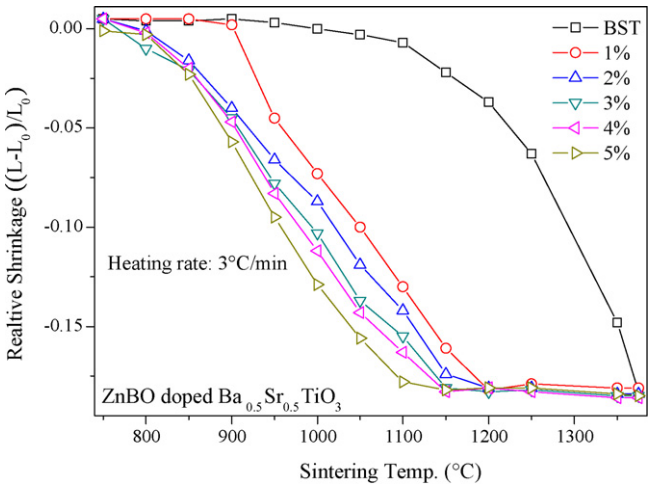

Fig. 1. Linear shrinkage as a function of temperature for $(Ba_{0.5}Sr_{0.5})TiO_3$ ceramic plates and 1–5 wt.% of ZnBO-doped $(Ba_{0.5}Sr_{0.5})TiO_3$ ceramic plates.

Therefore, the importance of ceramic materials, which have low-temperature sintering properties with the low-loss tangent become increased.

In this paper, we focused on the ZnBO for the low-temperature sintering aids for BST. We will discuss structural and electrical properties of ZnBO-doped BST ceramics for the LTCC applications.

2. Experimental

In this experiment, mixed powders of $Ba_{0.5}Sr_{0.5}TiO_3$ were prepared from $BaCO_3$, $SrCO_2$, and TiO_2 powders with high purity of 99.9% by conventional mixed oxide method. These powders were mixed with ZrO_2 balls for 24 h in alcohol. After drying, reagents were calcined at 1100 °C for 2 h and then slowly cooled. To fabricate the ZnBO dopants, ZnO and B_2O_3 (5:5) powders with high purity of 99.9% were mixed together. After being ball-milled for 24 h and dried, they were calcined at 800 °C for 2 h. This mixed powder was sieved to 100-mesh and then added in BST ceramics for reducing the sintering temperature of BST. After sieving the BST powders with 100 mesh, 1–5 wt.% of ZnBO were added to the BST powder to lower sintering temperature.

Respective compound powders were synthesized with ball milling and dried at the oven for 24 h and pressed into disks with 10 mm by 1 tonne/cm^2. These powders were respectively sintered from 750 to 1350 °C by 50 °C for 2 h to confirm the sintering temperature.

The crystalline structures of ZnBO-doped BST ceramics ware investigated by X-ray diffraction (XRD) pattern (θ–2θ scans with Cu Kα source). Frequency-dependent dielectric permittivity of these specimens was analyzed through *HP 4284 precision LCR meter* and *HP 4194A impedance analyzer*.

3. Results and discussion

Fig. 1 shows the linear shrinkage profiles of BST ceramic plates without and with 1, 2, 3, 4, and 5 wt.% of ZnBO. The ceramic plates were dried and made into a disk shape and then sintered from 750 to 1350 °C. The shrinkages of disks were measured after the sintering in order to investigate their shrinkage rates. By adding ZnBO to the BST, the onsets of the shrinkage of 2–5 wt.% ZnBO-doped BST were almost started at 750 °C but that of 1 wt.% ZnBO-doped BST was begun at 900 °C, which all specimens were drastically shrinked with increasing the temperature, whereas that of the BST without ZnBO was started at approximately 900 °C and slowly shrinked with increasing the temperature. The shrinkage rates of ZnBO-doped BST were different as increasing amount of ZnBO. Sintering process of ZnBO-doped BST was almost finished at 1100 °C. The 5 wt.% ZnBO-doped BST showed the highest shrinkage rate and was sintered at 1100 °C. In the case of 7 wt.% ZnBO-doped BST ceramic, which is not presented in this paper, the sintering temperature was not changed compared with that of 5 wt.% ZnBO-doped BST.

The densification kinetics is determined on the basis of Kingery's analysis for metal–ceramic composites. The shrinkage results obtained in Fig. 1 can be analyzed employing the following equations[10,11]:

$$\ln\left\{T\left[\frac{\mathrm{d}\Delta L/L_0}{\mathrm{d}T}\right]\right\} = \ln\left(\frac{1}{nK^{1/n}}\right) - \frac{1}{n}\ln\alpha - \frac{Q}{nRT} \quad (1)$$

where $\Delta L/L_0$ is the fractional shrinkage, T the absolute temperature, n the exponent, K the heating rate, Q the apparent activation energy and R is the gas constant. The n value is known to be in the range of 1.1–1.3. From Fig. 1, $\ln[T\,\mathrm{d}(\Delta L/L_0)/\mathrm{d}T]$ vs. $1/T$ results can be reconstructed in Fig. 2. By increasing the contents of ZnBO in BST, it seems the densification kinetic follows the Kingery's analysis. Straight line was fitted and their slopes were used to determine the apparent activation energy. As shown in the Fig. 2, the slopes of graph for 1, 2, 3 wt.% ZnBO-doped BST were different with that of BST. On the contrary, BST and 4, 5 wt.% ZnBO-doped BST have similar slope values. It means that sintering mechanism of 4, 5 wt.% ZnBO-doped BST is approximately similar to that of pure BST. The calculated activation energies of 4, 5 wt.% ZnBO-doped BST

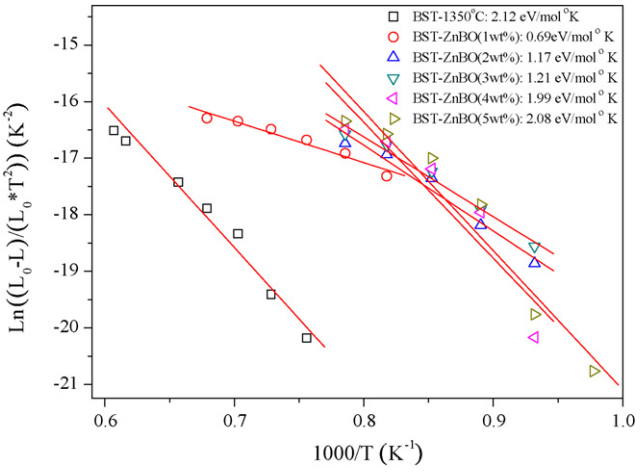

Fig. 2. Reconstructed curves showing kinetics for $(Ba_{0.5}Sr_{0.5})TiO_3$ ceramic plates and 1–5 wt.% of ZnBO-doped $(Ba_{0.5}Sr_{0.5})TiO_3$ ceramic plates.

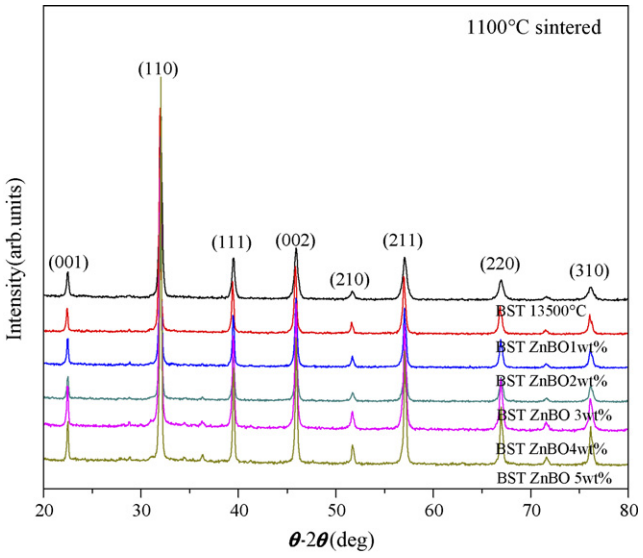

Fig. 3. XRD θ–2θ patterns of $(Ba_{0.5}Sr_{0.5})TiO_3$ ceramic plates sintered at 1350 °C and 1–5 wt.% of ZnBO-doped $(Ba_{0.5}Sr_{0.5})TiO_3$ ceramic plates sintered at 1100 °C.

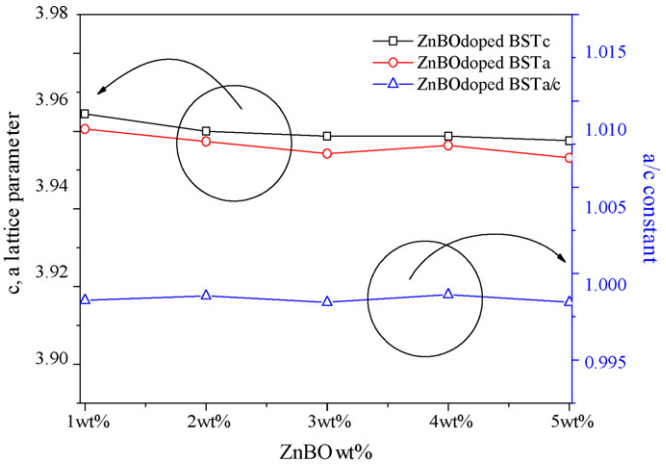

Fig. 4. Lattice parameters of a, c and the ratio of a/c of $(Ba_{0.5}Sr_{0.5})TiO_3$ ceramics with various ZnBO compositions.

were around 1.99 and 2.12 eV/mol K, and that of pure BST was about 2.12 eV/mol K.

Fig. 3 shows the X-ray θ–2θ patterns of BST sintered at 1350 °C and ZnBO-doped BST ceramic plates sintered at 1100 °C. As shown in the figure, these specimens show perovskite structure as same as that of BST sintered at 1350 °C and any pyro phase was not observed through XRD pattern analysis. Also the intensity of 5 wt.% ZnBO-doped BST was stronger than those of 1, 2, 3, 4 wt.% ZnBO-doped BST sintered at 1100 °C. The 1 1 0 reflection intensities of 5 wt.% ZnBO-doped BST and 1 wt.% ZnBO-doped BST are in the ratio of $I_{5\text{ wt.\% ZnBO-doped BST}}$:$I_{1\text{ wt.\% ZnBO-doped BST}} = 1.73$. Full width at half maximum (FWHM) of 5 wt.% ZnBO-doped BST in the reflection of (1 1 0) is 0.2°, while those of other specimens are larger than 0.22° (the tolerance of XRD equipment is about 0.003°). Therefore, it can be considered that by increasing the dopant of ZnBO to BST ceramic, specimens are well aligned with (1 1 0) orientations with narrow FWHM.

Fig. 4 displays lattice constants of c, a and lattice parameter ratio of a/c for ZnBO-doped BST ceramic plates. From the XRD θ–2θ scan in Fig. 3, lattice parameters of 1–5 wt.% of ZnBO-doped BST ceramics were calculated by employing *Nelson–Rilley* extrapolation function with least mean square methods. The equation can be expressed as follows:

$$\frac{C_{\cos\theta} - C_0}{C_0} = A\cos^2\theta\left(\frac{1}{\sin\theta} + \frac{1}{\theta}\right) \quad (2)$$

As shown in the figure by increasing the ZnBO contents, the lattice parameters of both c and a were decreased, however the weak tetragonality was remained. From the density of ZnBO-doped BST ceramics, by increasing the amount of ZnBO dopants, the density of ZnBO-doped BST was increased. The theoretical density of BST ceramic is 5.53 g/cm^3. The 5 wt.% ZnBO-doped BST ceramic has 95.4% of the theoretical density, while 1 wt.% ZnBO-doped BST ceramic has only 85.1%. We believe these decreased lattice parameters and high densities were probably related with compressive stress come from the high densification of ZnBO-doped BST ceramics with the grain agglomeration affects.[12]

Fig. 5 displays frequency dispersion of relative dielectric permittivity of ZnBO-doped BST in the frequency range from 1 kHz to 1 MHz. As shown in the Fig. 5, the relative dielectric permittivity of BST and ZnBO-doped BST ceramics have been reduced with increasing frequency from 1 kHz to 1 MHz. The relative dielectric permittivity of 1 wt.% ZnBO-doped BST decreased 0.68% from 1460 at 1 kHz to 1450 at 1 MHz, while the dielectric permittivity of 5 wt.% ZnBO-doped BST has decreased 1.0% from 1192 at 1 kHz to 1180 at 1 MHz.

Fig. 6 displays frequency dispersion of loss tangent of ZnBO-doped BST in the frequency range from 1 kHz to 1 MHz. As shown in the figure by adding ZnBO dopnat to BST, loss tangent of ZnBO-doped BST was decreased down to 27.9% compared with that of BST at 1 MHz. As a result, by comparing the

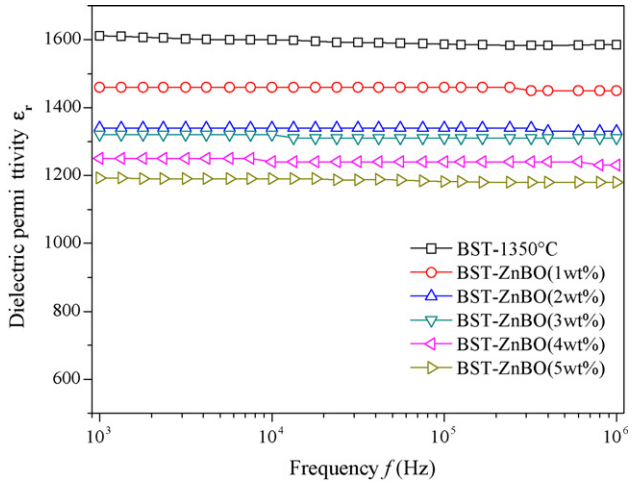

Fig. 5. Frequency-dependent relative dielectric permittivity of $(Ba_{0.5}Sr_{0.5})TiO_3$ ceramics sintered at 1350 °C and ZnBO-doped $(Ba_{0.5}Sr_{0.5})TiO_3$ ceramics sintered at 1100 °C measured from 1 kHz to 1 MHz at room temperature range with various ZnBO compositions.

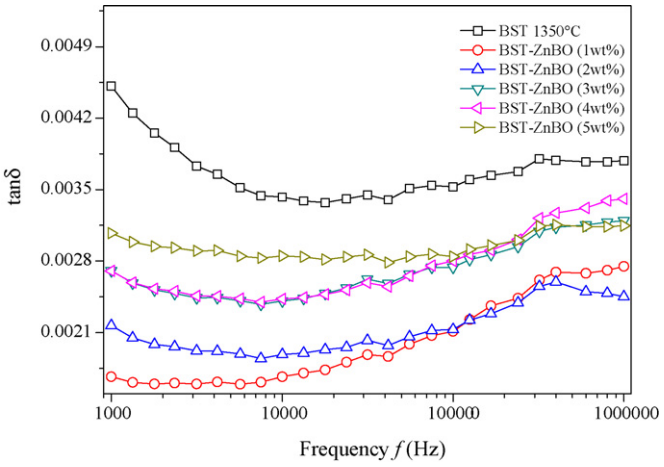

Fig. 6. Frequency-dependent loss tangent of $(Ba_{0.5}S_{0.5})TiO_3$ ceramics sintered at 1350 °C and ZnBO-doped $(Ba_{0.5}Sr_{0.5})TiO_3$ ceramics sintered at 1100 °C measured from 1 kHz to 1 MHz at room temperature range with various ZnBO compositions.

frequency dispersion from 1 kHz to 1 MHz, we found that 5 wt.% ZnBO-doped BST showed very weak dispersion of 9.37%. This frequency dispersion of 9.37% in 5 wt.% ZnBO-doped BST is even weaker than that of BST ceramics sintered at 1350 °C.

We believe this low-loss tangent of ZnBO-doped BST probably come from the increased density of ZnBO-doped BST ceramics due to the decreased porous area and increased grain size. This enlarged grain size with addition of ZnBO to the BST was confirmed at the SEM images of Fig. 7.

Fig. 7(a)–(e) show the SEM image of the 1–5 wt.% ZnBO-doped BST ceramic plates, respectively. By observing the grain shape and size of ZnBO-doped BST, we found that 1 wt.% ZnBO-doped BST has circular shape of grain with 1 μm of grain size, while 5 wt.% ZnBO-doped BST has rectangular shape with 6 μm of grain size. We may argue that this big grain size of 5 wt.% ZnBO-doped BST has related with completely well sintered material properties at 1100 °C as we have discussed in Fig. 3. It can be argued that by increasing the amount of ZnBO in BST, the grain size was increased and crystalline properties were improved.

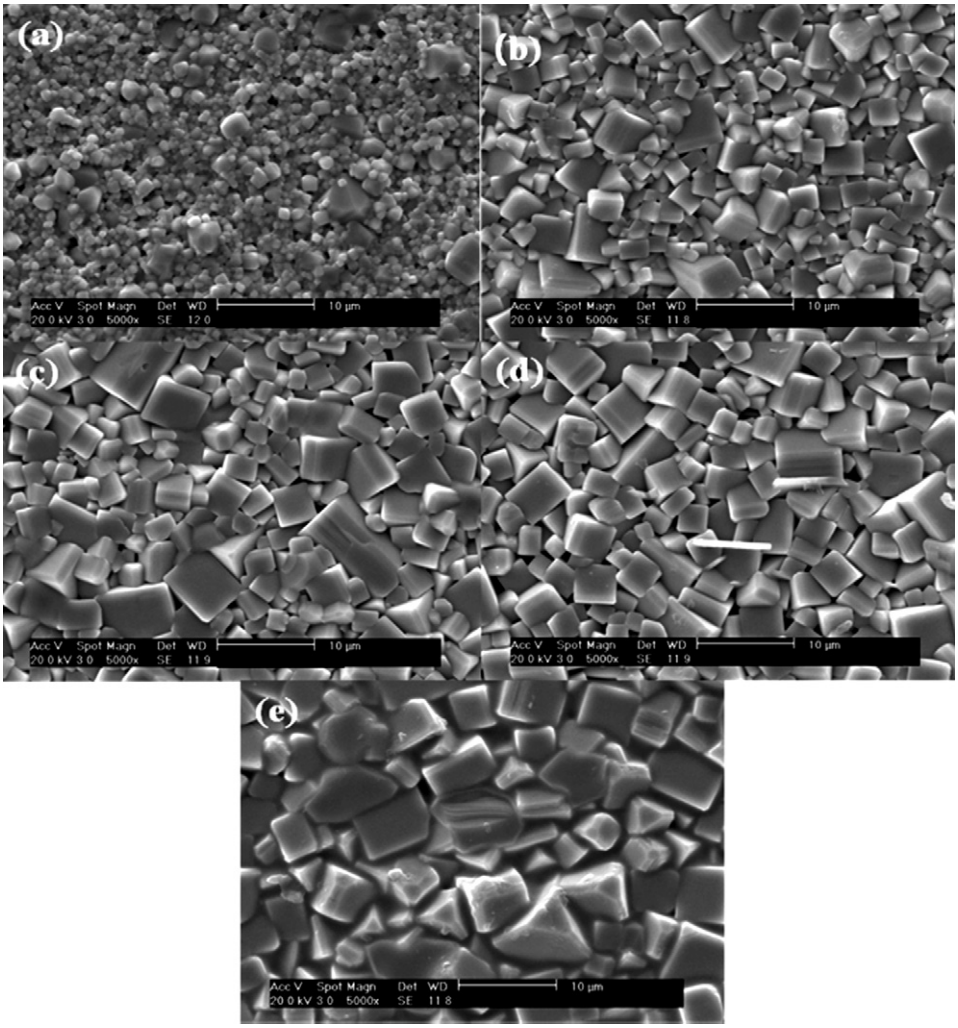

Fig. 7. SEM images of various wt.% of ZnBO-doped $(Ba_{0.5}Sr_{0.5})TiO_3$ ceramics sintered at 1100 °C for 2 h: (a) 1 wt.%, (b) 2 wt.%, (c) 3 wt.%, (d) 4 wt.%, and (e) 5 wt.%.

4. Conclusion

In this paper, we have investigated the fabrication and characterization of ZnBO-doped BST ceramics for LTCC applications. We have found that by adding the ZnBO to the BST the loss tangent was decreased from 3.07×10^{-3} to 2.78×10^{-3} by 9.37%, while relative dielectric permittivity was decreased from 1585 to 1180 by 22.5%. Sintering temperature of ZnBO-doped BST was decreased down to 1100 °C with relative dielectric permittivity of 1180 and loss tangent of 2.78×10^{-3}, respectively.

We may ascribe this low-loss tangent of ZnBO-doped BST to the increased density of ZnBO-doped BST ceramics and extensive grain size.

From the XRD analysis, we found that 1–5 wt.% ZnBO-doped BST have perovskite structure. The lattice parameters of *a*, *c*, and tetragonality were calculated and compared according to the ZnBO contents. From the SEM images, by increasing the ZnBO content to BST, grain size was increased and crystalline properties were improved.

Acknowledgment

This research has been supported by a grant form the Seoul Research and Business Development Program (Grant 10583).

References

1. Lim, J. B., Son, J., Nahm, S., Lee, W., Yoo, M., Gang, N. G. *et al.*, Low-temperature sintering of B_2O_3-added $Ba(Mg_{1/3}Nb_{2/3})O_3$ ceramics. *Jpn. J. Appl. Phys.*, 2004, **43**, 5388–5391.
2. Carlson, C. M., Rivkin, T. V., Parilla, P. A., Perkins, J. D. and Ginley, D. S., Large dielectric constant ($\varepsilon/\varepsilon_0 > 6000$) $Ba_{0.4}Sr_{0.6}TiO_3$ thin films for high-performance microwave phase shifters. *Appl. Phys. Lett.*, 2000, **76**, 1920–1922.
3. Outzourhit, A., Trefny, J. U., Kito, T. and Yarar, B., Tunability of the dielectric constant of $Ba_{0.1}Sr_{0.9}TiO_3$ ceramics in the paraelectric state. *J. Mater. Res.*, 1995, **10**, 1411–1417.
4. Zimmermann, F., Voigts, M., Weil, C., Jakoby, R., Wang, P., Menesklou, W. *et al.*, Investigation of barium strontium titanate thick films for tunable phase shifters. *J. Eur. Ceram. Soc.*, 2001, **21**, 2019–2023.
5. Hwang, S. and Kim, H., Effect of frit size on microwave properties of glass–ceramic in low temperature co-fired ceramics. *Thermochim. Acta*, 2007, **455**, 119–122.
6. Huang, C.-L., Lin, R.-J. and Wang, J.-J., Effect of B_2O_3 additives on sintering and microwave dielectric behaviors of CuO-doped $ZnNb_2O_6$ ceramics. *Jpn. J. Appl. Phys.*, 2002, **41**, 758–762.
7. Wang, X., Murakami, K. and Kaneko, S., High-performance $PbZn_{1/3}Sb_{2/3}O_3$–$PbNi_{1/2}Te_{1/2}O_3$–$PbZrO_3$–$PbTiO_3$ ceramics sintered at a low temperature with the aid of complex additives Li_2CO_3–Bi_2O_3–$CdCO_3$. *Jpn. J. Appl. Phys.*, 2000, **39**, 5556–5559.
8. Lee, H. R., Yoon, K. H. and Kim, E. S. O., Low temperature sintering and microwave dielectric properties of $BiNbO_4$–$ZnNb_2O_6$ ceramics with CuV_2O_6 additive. *Jpn. J. Appl. Phys.*, 2003, **42**, 6168–6171.
9. You, H. W. and Koh.F J.H., Structural electrical properties of low temperature sintered Li_2CO_3 doped (Ba, Sr)TiO_3 ceramics. *Jpn. J. Appl. Phys.*, 2006, **45**, 6362–6364.
10. Jean, J. H. and Gupta, T. K., Isothermal and nonisothermal sintering kinetics of glass-filled ceramics. *J. Mater. Res.*, 1992, **7**, 3342–3347.
11. Zuo, R., Li, L., Gui, Z., Hu, X. and Ji, C., Effects of additives on the interfacial microstructure of cofired electrode-ceramic multilayer systems. *J. Am. Ceram. Soc.*, 2002, **85**, 787–793.
12. German, R. M. and Olevsky, E. A., Modeling grain growth dependence on the liquid content in liquid-phase-sintered materials. *Metall. Mater. Trans. A*, 1998, **29**, 3057–3067.